

See discussions, stats, and author profiles for this publication at: <https://www.researchgate.net/publication/229897731>

# Effect of Architecture in the Surface Segregation of Polymer Blends

ARTICLE *in* MACROMOLECULES · NOVEMBER 1996

Impact Factor: 5.8 · DOI: 10.1021/ma9602278

---

CITATIONS

42

---

READS

18

## 2 AUTHORS:



David Wu

Colorado School of Mines

98 PUBLICATIONS 1,666 CITATIONS

[SEE PROFILE](#)



Glenn H Fredrickson

University of California, Santa Barbara

434 PUBLICATIONS 28,369 CITATIONS

[SEE PROFILE](#)

# Effect of Architecture in the Surface Segregation of Polymer Blends

David T. Wu<sup>\*,†</sup> and Glenn H. Fredrickson

Departments of Chemical Engineering and Materials, University of California,  
Santa Barbara, California 93106

Received February 13, 1996; Revised Manuscript Received August 12, 1996<sup>‡</sup>

**ABSTRACT:** We examine the surface segregation behavior of binary polymer blends with architecturally asymmetric components. Particular attention is given to molten blends containing linear and branched polymers composed of the same type of monomer. If the branches are sufficiently long and the branch points (joints) dilute, we argue that the surface enrichment behavior has universal features that are independent of the chemical identity of monomers. We identify entropic and enthalpic contributions to the surface potentials acting on end, joint, and middle monomers of each species and show that these can be incorporated into a linear response formalism for the prediction of surface enrichment. Applications to linear-comb and linear-star mixtures are explicitly demonstrated, and scaling relations for the integrated surface enrichment and enrichment length scale are identified. We also identify a topological enrichment mechanism for blends that contain loops, e.g. linear-ring mixtures. Surprisingly, a dilute amount of ring polymer added to a linear melt is found at a surface at precisely twice the bulk concentration, independent of ring length. This is argued to be a natural consequence of the reflecting boundary conditions that are imposed on polymer propagators for nearly incompressible melts at impenetrable surfaces.

## I. Introduction

Techniques for surface modification of plastics have become extremely important in a number of modern technologies. These techniques may be chemical, in which reactions are used to functionalize or transform the surface layer, or physical, in which surface-active agents (e.g. copolymers) are placed at a surface and allowed to self-assemble, exposing a specific chemical functionality. A related type of self-assembly is the subject of the present paper. Because many important commercial thermoplastics are actually blends, there is considerable interest in the surface segregation behavior of molten polymer mixtures, i.e., the extent to which the composition of the blend in the surface layer differs from that in the bulk. By developing an understanding of the structural, chemical, and architectural features that control surface segregation, it might be possible to exert control over surface properties in the melt state and preserve or exert further control during subsequent cooling and structural arrest.

A number of factors evidently relate to the enrichment of one component near a surface in molten polymer blends. From a *macroscopic* perspective, and in the absence of surface-specific interactions (of either an enthalpic or entropic nature), the surface of a binary (A–B) blend will generally be enriched in the component with the smaller pure-component surface free energy (i.e., tension). The difference in surface free energies,  $\gamma_A - \gamma_B$ , serves as a “surface field” that acts on the composition variable in the surface layer. In a miscible blend, the tendency of this field to produce a surface layer rich in the lower  $\gamma$  component is opposed by the osmotic (thermodynamic) forces that drive mixing in the bulk of the melt. The balance of these competing forces is responsible for both the amplitude (i.e., deviation of the surface composition from the bulk composition) and the scale (i.e., the depth of penetration of the surface-

enriched layer) of surface segregation in miscible blends. In immiscible blends, these same factors are instrumental in dictating wetting behavior.<sup>1</sup>

From a *microscopic* perspective, both energetic and entropic factors contribute to the “surface field”, as well as to the osmotic restoring forces. The presence of a surface can induce segregation, due to differential coupling of the surface to one of the two components. This coupling can be to various aspects, enthalpic and entropic, of the surface structure. However, the common, defining characteristic of a surface is that the density drops from its bulk value to nearly zero. Generically, at a free (air or vacuum) surface of a melt, one expects this profile to be a smooth drop, characteristically over the length scale of a few monomers. As has been pointed out recently,<sup>2</sup> the existence of this depletion region leads to a favorable coupling of the surface to the component with the lower value of the pure-component parameter  $\beta^2 = R_g^2/V$  ( $R_g$  and  $V$  are the radius of gyration and chain molecular volume, respectively), related to the conformational entropy of chains near a surface. A smooth depletion profile may also describe surfaces near solids under certain conditions (e.g., when the bulk cohesive forces are stronger than attractions to the surface, or at lower polymer densities<sup>3</sup>); conversely, even for free surfaces, there may not be a smooth depletion region if, for example, there is a strong hydrogen-bonding network that terminates in a sharp, lattice-like manner at the surface. We note that the surface can in addition couple to other aspects of the polymer structure: for instance, a hard, flat surface can induce layering or orientational ordering, thereby favoring the component that can pack itself better, or orient itself more easily, near the surface. Nonetheless, to the degree that the structure of the surface is similar to that of a free surface, the surface will be enriched with the component having the lower (free) surface tension.

Thus, at a low-energy surface, such as air or vacuum, the component with lowest cohesive energy density is generally favored,<sup>3</sup> since the potential energy cost of separating the melt and producing surface is minimized.

<sup>\*</sup> New address: Departments of Chemistry and Chemical Engineering, Colorado School of Mines, Golden, CO 80401.  
<sup>†</sup> Abstract published in *Advance ACS Abstracts*, October 15, 1996.

However, as mentioned above, the surface tension can also contain a factor depending on the conformational entropy related parameter  $\beta$ . (We stress here that, in this mechanism, even when it is the difference in the *conformational entropies* of the components that determines which is the preferred species, the magnitude of the effect reflects a balance of both entropic and enthalpic considerations,<sup>2,4</sup> and so has been termed *entropically mediated*.<sup>5a</sup>) In polyolefin blends at air surfaces<sup>6</sup> and in polyolefin diblock copolymers near solid and air surfaces,<sup>7</sup> both of these factors favor surface enrichment by the more highly branched (lower  $\beta$ ) component. Increasing the level of short-chain branching (e.g. butene or octene branches) tends to frustrate packing in the bulk liquid, thereby lowering the cohesive energy density and solubility parameter, but also lowers the entropic parameter  $\beta$ . For polyolefin random copolymer blends, no segregation is observed at a *solid* surface,<sup>6</sup> suggesting that entropically mediated factors related to the local *packing* and *tiling* of monomers of different sizes and shapes near a surface may eliminate the depletion region, and thus be dominant there. This interpretation has been corroborated by simulations and polymer-RISM theory on athermal tangent hard-sphere chains near perfectly flat hard walls.<sup>5a,b</sup>

In contrast, the experiments on model polyolefin diblock copolymers surprisingly show enrichment by the smallest  $\beta$  block at solid surfaces, even at high energy surfaces (i.e., surfaces composed of materials with cohesive energy densities higher than polyolefins). In such circumstances, one might expect a competition whereby the olefin with the highest cohesive energy density is preferred at the surface for energetic reasons, while the low- $\beta$  block is again favored for entropic reasons. The experimental observation that the "smallest  $\beta$  rule" is apparently universally obeyed for the surfaces of polyolefin diblock copolymers seems to suggest the dominance of the conformational entropy factor in determining the sign of enrichment for such materials. While a molecular mean-field theory of Carignano and Szleifer<sup>5c</sup> finds additionally that bending stiffness of chains acts to favor stiff chains at a surface due to nematic-like tiling at a flat hard wall (as may be a consideration for blends), these effects apparently do not control the sign of segregation in diblocks, either in their theory or in experiments. We emphasize that these issues are relevant to short-branched polymers, where there are several competing effects on the monomer scale, and are discussed elsewhere;<sup>4,5a</sup> as they do not bear directly on the question of universal behavior of long-branched polymers considered here, we will not consider them further in this paper.

In *bulk* mixtures of polymers, we have recently argued<sup>8</sup> that an excellent way to isolate contributions to the excess free energy of mixing associated with conformational entropy effects and eliminate packing effects is to focus on blends whose components are composed of the same type of monomer, but differ in the degree of *long-chain branching* (i.e., "architecturally asymmetric" blends). Such blends are not restricted to the class of polyolefin materials, but might include, for example, mixtures of linear and star or comb-shaped polystyrenes. Because the dominant contribution to the excess free energy in such mixtures is associated with conformational entropy on length scales comparable to the size of the long branches ( $\approx 50-100 \text{ \AA}$ ) and much larger than monomer size scales ( $\approx 1-5 \text{ \AA}$ ), the thermodynamics of such mixtures has a high degree of

*universality*, i.e., insensitivity to the types of monomers composing the polymeric components. A recent theoretical study<sup>9</sup> extended the formalism to examine the interfacial thermodynamics of *internal* interfaces in such systems, e.g. between a phase rich in linear polystyrene and a phase rich in comb-shaped polystyrene. A high degree of universality was found for both the interfacial tension and the composition profile between coexisting phases.

In the present paper, we explore the interfacial thermodynamics of architecturally asymmetric blends at *external* interfaces (i.e., surfaces). By restricting attention to mixtures with components that differ only in the degree and placement of long branches, we can again eliminate local packing effects and thereby identify universal aspects of surface segregation that are associated with conformational entropy related to gross architectural differences between blend components. Such insights could prove very valuable in the design and manipulation of polymer surface properties.

Our strategy for describing mixtures of branched and linear polymers is to consider first the distribution and configurations of a single (i.e., dilute) branched polymer in a melt of very long linear chains at a surface. (Throughout, we adopt a mean-field description of chain statistics and work within the framework of self-consistent field theory pioneered by Edwards and Helfand.<sup>10-12</sup>) In this limiting situation, the density profile is given within a ground-state approximation which serves as a coarse-grained representation of a depletion layer. Building upon our previous work on linear homopolymer melts,<sup>2,13</sup> we demonstrate that the ground-state density profile induces chain statistics for the branched polymer consistent with reflecting boundary conditions augmented by surface potentials for ends and joints. These surface potentials, however, are thereafter treated as phenomenological parameters, since they can in practice be supplemented by other contributions to the surface field of enthalpic or entropic origin. Nonetheless, the above dilute limit, which can be solved analytically, then serves as a reference system for calculating surface composition profiles of arbitrary mixtures of branched and linear polymers within linear response theory. Next, we make a connection between the present analysis for long-branched blends and previous work<sup>2</sup> on short-branched blends (modeled as linear chains with effective  $\beta$  parameters) by examining our results for combs in the coarse-grained limit that the teeth are much shorter than the backbone. In the final section, we examine surface segregation in blends of linear chains with rings or other loop-containing polymers.

## II. Dilute Branched Polymer Additives in a Melt of Long Linear Chains

In the present section, we consider a melt of long linear chains, which we label L, to which is added a dilute amount of a branched polymer species, which we label B. We discuss first the case where the added species is dilute enough that we can consider one molecule of B at the surface at a time. Furthermore, we restrict ourselves to the case where the B molecule has no internal loops; i.e., any pair of monomers chosen are connected by a unique path along the branched polymer (the effect of loops will be handled separately in a later section). Otherwise, our analysis will apply to any branched architecture, but for reasons of clarity and relevance to industrial materials, we focus on two

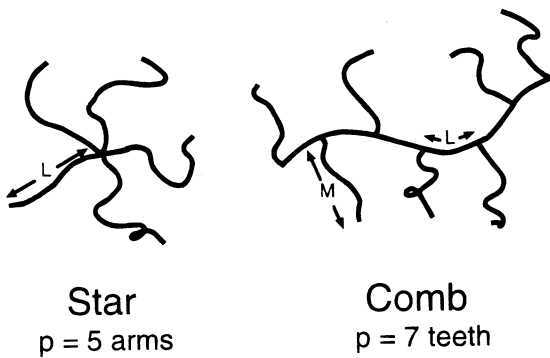


**Figure 1.** Depiction of a star polymer ( $p$  arms of length  $L$ ) and a comb polymer ( $p$  teeth of length  $M$  separated by lengths  $L$  along the backbone).

types of common branched polymers: stars and combs, which are represented schematically in Figure 1. The architecture of a star polymer (to which we assign the value  $S$  to the label B) is characterized by the number of arms,  $p$ , each consisting of  $L$  monomers that radiate from a central joint. A comb polymer (to which we assign the value  $C$  to the label B) has  $p$  evenly spaced teeth, each containing  $M$  monomers, and separated by  $L$  monomers between junction points (which we also call joints) where the teeth attach to the backbone. The linear chains that comprise the background melt are each  $N$  monomers long.

The monomers that constitute the branched polymers are considered to be identical to those forming the linear polymers and have a statistical segment length  $b$  and volume  $v_m$ . In the present study, we do not include a bulk Flory  $\chi$  interaction parameter (which can for example arise from entropic considerations of composition fluctuations<sup>8,15</sup>) between linear and branched components. Nonetheless, the end and joint monomers on any of the polymer molecules may be chemically different from the middle monomers. Assuming that the polymer conformations obey Gaussian statistics under melt conditions, we take the Hamiltonian for the polymers to be given by the sum of two contributions. The first is a Gaussian chain part (we choose energy units of  $k_B T$ )

$$H_0[\mathbf{R}_{i,\alpha}(s)] = \frac{3}{2b^2} \sum_{i,\alpha} \int_0^{N_\alpha} ds \left( \frac{d\mathbf{R}_{i,\alpha}(s)}{ds} \right)^2 \quad (2.1)$$

where  $\mathbf{R}_{i,\alpha}(s)$  is the position of monomer  $s$  on “piece”  $\alpha$  of polymer molecule  $i$ . By “piece”, we mean either a backbone, a tooth, or an arm (i.e., the linear chain has only a backbone, while a star has only arms, and a comb has both a backbone and teeth). The integration interval is therefore given by the length  $N_\alpha$  of the “piece”. (The label  $\alpha$  also distinguishes between the comb backbone and the backbone of the linear chain. Additionally, “pieces” are defined such that the entire polymer molecule remains connected.) The second part of the Hamiltonian represents a coarse-grained description of interactions

$$H_{\text{int}}[\hat{\rho}(\mathbf{r})] = \frac{1}{2} v \int d\mathbf{r} \hat{\rho}(\mathbf{r})^2 \quad (2.2)$$

as a functional of the microscopic density

$$\hat{\rho}(\mathbf{r}) = \sum_{i,\alpha} \int_0^{N_\alpha} ds \delta(\mathbf{r} - \mathbf{R}_{i,\alpha}(s)) \quad (2.3)$$

This simplistic excluded-volume-like description, used previously for homopolymer concentrated solutions,<sup>12,14</sup> melts,<sup>13</sup> and blends<sup>2,10,11,14</sup> of linear polymers, represents a harmonic penalty for fluctuations about the bulk density, and so should be accurate for small fluctuations. We note, however, that the parameter  $v$  cannot be naively taken to be simply an excluded-volume parameter. Rather, it represents a coarse-grained local effective interaction (direct-correlation function), and can be related to the finite compressibility of the melt. We also add the caveat that near a surface, where the profile deviates significantly from its bulk value, a quadratic free-energy functional is insufficient to provide a quantitative description of the profile. Nonetheless, in the coarse-grained spirit of this work, as in ref 12, the salient qualitative feature is the depletion shape of this surface profile, the width of which can be roughly related to the penalty for incurring density fluctuations. The reader is referred to refs 10–13 for further discussion of the validity of this coarse-grained description.

Within mean-field theory, the conformations of the branched polymers are given by Gaussian statistics acting in the self-consistent potential  $U(\mathbf{r}) = v\rho(\mathbf{r})$ , where  $\rho(\mathbf{r})$  is the mean monomer density field. In particular, the Green’s function for observing monomer  $s$  at point  $\mathbf{r}$  and monomer  $s'$  at point  $\mathbf{r}'$  is given by<sup>12</sup>

$$G(\mathbf{r}, \mathbf{r}'; s, s') = \int \mathcal{D}\mathbf{R}(s^*) e^{-\{H_0[\mathbf{R}(s^*)] + \int ds U(\mathbf{R}(s^*))\}} \times \delta(\mathbf{R}(s) - \mathbf{r}) \delta(\mathbf{R}(s') - \mathbf{r}') / \int \mathcal{D}\mathbf{R}(s^*) e^{-H_0[\mathbf{R}(s^*)]} \delta(\mathbf{R}(s) - \mathbf{r}) \quad (2.4)$$

where the path integral is performed over paths  $\mathbf{R}(s^*)$  with  $s^*$  on the unique sequence connecting  $s$  and  $s'$ . Since the dependence on  $s$  and  $s'$  enters only as the number of monomers separating them along their connecting path, the Green’s function is simply that of a linear chain with  $|s - s'|$  intervening monomers, calculated in the same potential.

For dilute enough concentrations of branched B polymers, the monomer density profile is dominated by the density of monomers on linear chains. For large enough  $N$ , this density profile approaches a limit that can be described by the “ground-state” approximation<sup>10</sup>

$$\rho_{\text{GS}}(z) = \rho_b Q^2(z) \quad (2.5)$$

where  $\rho_b$  is the bulk monomer density, and

$$Q(z) \equiv \int d\mathbf{r}' G(\mathbf{r}, \mathbf{r}'; s, s') = \tanh(z/\xi) \quad (2.6)$$

is a reduced partition function in the ground-state limit of  $|s - s'|^{1/2}b \gg \xi$ . In the above,  $z$  is the component of  $\mathbf{r}$  normal from the surface,  $\xi$  is the bulk screening length defined by

$$\xi = \frac{b}{(3v\rho_b)^{1/2}} \quad (2.7)$$

and we have taken the zero of potential to be in the bulk at  $z = \infty$ . Physically,  $\xi$  represents the length scale on which the total monomer density “heals” from zero at the wall to the bulk value  $\rho_b$  at  $z = \infty$ . The density profile for finite  $N$  is similar, with corrections entering only at order  $\mathcal{O}(1/N)$ .<sup>13</sup> Moreover, the monotonic rise of eq 2.5 (as opposed to a more realistic oscillatory profile in fluids with sharply repulsive short-ranged potentials)

is a consequence of our coarse-grained quadratic model of interactions, eq 2.2.

### III. Reflecting Boundary Conditions with Effective Surface Potentials for Ends and Joints

The above form of the potential  $U(z) = v\rho_{GS}(z)$  implied by eq 2.5 allows an exact evaluation of the Green's function as defined by eq 2.4. In the limit of intervening (linear) stretches of chain much larger than the width of the interfacial or surface layer, i.e.,  $|s - s'|^{1/2}b \gg \xi$ , this Green's function has been shown previously<sup>13</sup> to approach

$$G(z, z'; s, s') \approx Q(z)G_{\text{refl}}(z, z'; s, s')Q(z') \quad (3.1)$$

where  $G_{\text{refl}}$  is the Green's function for reflecting boundary conditions

$$G_{\text{refl}}(z, z'; s, s') = \left( \frac{3}{2\pi|s - s'|b^2} \right)^{1/2} \times [e^{-3(z-z')^2/2|s-s'|b^2} + e^{-3(z+z')^2/2|s-s'|b^2}] \quad (3.2)$$

in the absence of the potential. The meaning of reflecting boundary conditions is simply that beyond a distance of the width of the surface,  $\xi$ , the chains have local conformations that are the same as in the homogeneous bulk (i.e., the surface is screened). The  $Q$  factors in eq 3.1 can be interpreted as exerting a surface potential for ends,<sup>13</sup> which we recapitulate as follows: From the Green's function above, it is possible to arrive at the surface profiles for either the total monomer density or the density of end monomers only. When coarse-grained over the length  $\xi$ , these profiles are found within linear response to be precisely those produced by a selective surface potential for ends acting on polymers otherwise obeying pure reflecting boundary conditions. This surface potential is of entropic origin and can be expressed as

$$-T\Delta s_e = -c_1\xi k_B T \delta(z - 0^+) \quad (3.3)$$

where the numerical constant for ends is  $c_1 = 1 - \ln(2)$ . Note that the strength of the potential is also consistent (within linear response) with the ground-state value for the integrated surface excess of end monomers (per unit area)

$$\int_0^\infty dz \left[ \rho_{\text{ends}}(z) - \frac{2}{N} \rho(z) \right] = \int_0^\infty dz \frac{2\rho_b}{N} [Q(z) - Q^2(z)] = \frac{2}{N} \rho_b c_1 \xi \quad (3.4)$$

when the ends are considered as a free (ideal gas) species, i.e., having a response function  $S(z) = (2\rho_b/N)\delta(z)$ .

The above analysis can be generalized to obtain an entropic surface potential for joints. The magnitude of the surface potential for joints is given by the free energy for bringing a joint to the surface region. We imagine, therefore, a joint with  $p$  arms, each long enough so that any memory of positional information from the other end is lost. In this case, the probability density of finding the joint at position  $z$  is proportional to the probability of an arm ending (connecting) at the position of the joint,  $\sim Q(z)$ , happening  $p$  independent times, and is thus given by

where  $\rho_{jb}^B$  is the bulk density of joint monomers. (We have neglected in our Gaussian model correlations between different arms, which are screened beyond a distance of order  $\xi$ .) For a depletion layer,  $Q(z) < 1$  near the surface, and hence joints are effectively repelled from the surface relative to other monomers. Within linear response, the strength of the effective potential is proportional to the response, i.e., the amount of relative excess, which is (up to normalization factors)

$$c_p = \int_0^\infty [\tanh^p(z) - \tanh^2(z)] dz \approx -\frac{1}{2} \ln\left(\frac{p}{2}\right) \quad (3.6)$$

The resulting coarse-grained effective potential relative to monomers in the middle of a linear chain can then be written

$$-T\Delta s_j = -c_p \xi k_B T \delta(z - 0^+) \quad (3.7)$$

It is important to note that the strength of the effective potential also scales linearly with the screening length  $\xi$ . The approximation in eq 3.6 (which is asymptotic for  $p \rightarrow \infty$ ) is good to within 5% for  $p \geq 2$ , and deviates by less than 15% for  $p = 1$ . Essentially, we find that the ends are sticky (attractive), while the joints experience a repulsion that grows logarithmically with the number of arms. Therefore for a star or comb polymer as a whole (or for other branched polymers with more ends than joints), this entropic surface attraction for ends dominates over the repulsion for joints.

There is usually, however, some chemical difference between end, joint, and middle monomers, resulting for example from initiation, termination, or other synthesis-related processes. Even in the case of pure hydrocarbon polyolefins, there exists some differential enthalpic surface interaction for the terminal  $\text{CH}_3$  group as compared to that of the middle methylene  $\text{CH}_2$  groups.<sup>16</sup> For the remainder of the paper, we shall therefore consider the surface potentials to be phenomenological parameters. In particular, they are assumed to accommodate different origins of free energy differences for placing ends or joints versus middle monomers at the surface. Differential enthalpic interactions with the surface,  $\Delta h_e$  or  $\Delta h_j$ , can then simply be added to the entropic potentials,  $-T\Delta s_e$  or  $-T\Delta s_j$ , calculated above to give effective surface fields

$$U_e^B(\mathbf{r}) = U_e^B \delta(z) \equiv \Delta \mu_e = \Delta h_e - T\Delta s_e$$

$$U_j^B(\mathbf{r}) = U_j^B \delta(z) \equiv \Delta \mu_j = \Delta h_j - T\Delta s_j \quad (3.8)$$

for ends and joints of branched polymers, respectively. Other possible significant differences of entropic origin include steric or packing effects (for example due to different joint/end group shape or size) or a contribution due to the stiffness of the chain.<sup>18</sup> We emphasize that even with such contributions, as long as the pieces of the polymers (between joints) are long enough to obey coarse-grained Gaussian statistics, these effects can be included within our description of a Gaussian polymer interacting with a surface potential.

**Density Profiles of Dilute Branched Additives.** For sticking energies that are not too large, we can use linear response theory to calculate the density profiles of the branched polymers at the surface. (The linear response estimate should be accurate so long as the

relative composition changes, which diminish with chain length, are not too large compared to unity; we discuss this further below.) Since the effective surface potentials act on ends and joints, the change in the density of B monomers is given by

$$\Delta\rho^B(\mathbf{r}) = -\int d\mathbf{r}' [S_{pe}^B(\mathbf{r}, \mathbf{r}') U_e^B(\mathbf{r}') + S_{pj}^B(\mathbf{r}, \mathbf{r}') U_j^B(\mathbf{r}')] \quad (3.9)$$

which follows from our analysis of the Green's function, eq 3.1, as producing an entropic surface potential for ends and joints, supplemented by any enthalpic surface interactions. In the above, the density/end density and density/joint density response functions for the branched polymer are given respectively by

$$\begin{aligned} S_{pe}^B(\mathbf{r}, \mathbf{r}') &= \langle \delta\rho^B(\mathbf{r}) \delta\rho_e^B(\mathbf{r}') \rangle \\ S_{pj}^B(\mathbf{r}, \mathbf{r}') &= \langle \delta\rho^B(\mathbf{r}) \delta\rho_j^B(\mathbf{r}') \rangle \end{aligned} \quad (3.10)$$

In addition, we will later need the branched monomer density/density response function

$$S_{pp}^B(\mathbf{r}, \mathbf{r}') = \langle \delta\rho^B(\mathbf{r}) \delta\rho^B(\mathbf{r}') \rangle \quad (3.11)$$

Equation 3.9 results from considering the surface as interacting with only one end (or joint) at a time, although we average over all possible interactions.

The branched polymer response functions above are defined using the reflecting boundary condition Green's function to calculate configurational averages. However, since the perturbing potential is situated at the origin, it is convenient to consider eq 3.9 equivalently as the convolution of the free response functions (i.e., configurational averages taken in a flat infinite space) with the sum of the original perturbing potential and its reflected image (i.e., double the original potential).<sup>17</sup> To prove this equivalence, we consider a generic response formula

$$\Delta\rho(z) = -\int_0^\infty dz' S(z, z') U(z'), \quad z > 0 \quad (3.12)$$

We are free to make an even extension of  $\Delta\rho$  to the (unphysical) left half-plane  $z < 0$ , which allows us to write

$$\begin{aligned} \Delta\rho(z) &= \frac{1}{2} [\Delta\rho(z) + \Delta\rho(-z)] \\ &= -\frac{1}{2} \int_0^\infty dz' S(z, z') U(z') - \\ &\quad \frac{1}{2} \int_0^\infty dz'' S(-z, z'') U(z'') \end{aligned} \quad (3.13)$$

We also choose an even extension for both  $U(z)$  and  $S(z, z')$  to the left half-plane [ $U(z) = U(-z)$ ;  $S(z, z') = S(-z, -z')$ ], which with the change of variables  $z' = -z''$  in the second integral leads to

$$\Delta\rho(z) = -\frac{1}{2} \int_{-\infty}^\infty dz' S(z, z') U(z') \quad (3.14)$$

Next, we note that  $S(z, z')$  satisfying reflecting boundary conditions can be written as

$$S(z, z') = S_{free}(z, z') + S_{free}(z, -z') \quad (3.15)$$

where  $S_{free}(z, z')$  is the corresponding free-space propagator. That the above is true for a branched polymer can

be seen as follows. The response function for a given arbitrary pair of monomers on a branched polymer can be expressed as a product of Green's functions of the form  $G_{refl}(z, z'; s, s')$  representing the weight of all the "pieces" of the polymer (including the "pieces" defined as ending at one of the pair of monomers). As postulated, there is a single linear path that connects these two chosen monomers. All the other pieces have one end free. However, the associated weight for integrating over the reflecting boundary condition Green's function for a chain with a free end is a constant, i.e., homogeneous in space. The final weight for the two chosen monomers is then simply proportional to the reflecting boundary condition Green's function for the interconnecting linear piece. After normalization and summation over monomers, we recover eq 3.15.

Substitution into eq 3.14 leads to

$$\Delta\rho(z) = -\int_{-\infty}^\infty dz' S_{free}(z, z') U(z') \quad (3.16)$$

Our final step is to note the form of  $U(z)$ , subsequent to extension to  $z < 0$ :

$$U(z) = U\delta(z - 0^+) + U\delta(z - 0^-) \quad (3.17)$$

Fourier transformation (denoted by a hat, and with transform variable  $k$ ) thus yields

$$\hat{\Delta\rho}(k) = -\hat{S}_{free}(k) 2U \quad (3.18)$$

which completes our proof of the above stated equivalence.

Next, we tabulate the Fourier transforms of the free response functions for the branched polymers discussed in this paper. The density/density and density/end density response functions for a linear polymer are

$$\begin{aligned} \hat{S}_{pp}^L(k) &= N(1-f)\rho_b g_D(Nk^2 b^2/6) \\ \hat{S}_{pe}^L(k) &= 2(1-f)\rho_b g_e(Nk^2 b^2/6) \end{aligned} \quad (3.19)$$

where

$$g_D(x) = \frac{2}{x^2} (e^{-x} - 1 + x) \quad (3.20)$$

is the familiar Debye function,

$$g_e(x) = \frac{1}{x} (1 - e^{-x}) \quad (3.21)$$

is a Debye-like function for ends, and  $f$  is the fraction of all monomers that are from B molecules.

For stars, the response functions are

$$\hat{S}_{pp}^S(k) = f\rho_b L[g_D(Lk^2 b^2/6) + (p-1)g_e^2(Lk^2 b^2/6)]$$

$$\hat{S}_{pe}^S(k) = f\rho_b g_e(Lk^2 b^2/6)[1 + (p-1)\exp(-Lk^2 b^2/6)]$$

$$\hat{S}_{pj}^S(k) = f\rho_b g_e(Lk^2 b^2/6) \quad (3.22)$$

and finally,

$$\hat{S}_{\rho\rho}^C(k) = f\rho_b \left( \frac{6}{k^2 b^2} \right)^2 \left\{ 2(p-1) \left[ \left( \frac{k^2 b^2}{6} \right) (L+M) + \frac{(1-lm)(1-m)}{1-l} \right] + \left[ \left( \frac{k^2 b^2}{6} \right)^2 g_D(Mk^2 b^2/6) - 2 \left( \frac{1-lm}{1-l} \right)^2 (1-l^{p-1}) \right] \right\}$$

$$\hat{S}_{\rho e}^C(k) = f\rho_b \left( \frac{6}{k^2 b^2} \right) \left\{ p \left[ (1-m) + \frac{2m(1-lm)}{1-l} \right] - \frac{2m(1-lm)}{(1-l)^2} (1-l^p) \right\}$$

$$\hat{S}_{\rho j}^C(k) = f\rho_b \left( \frac{6}{k^2 b^2} \right) \left\{ p \left[ (1-m) + \frac{2(1-lm)}{1-l} \right] - \frac{2(1-lm)}{(1-l)^2} (1-l^p) \right\} \quad (3.23)$$

are the response functions for combs, where for notational convenience we have written  $l = \exp(-Lk^2 b^2/6)$  and  $m = \exp(-Mk^2 b^2/6)$ . For the comb response functions, we have organized the expressions into a first term which scales with  $p$ , and a second term which represents corrections for end effects. We note, however, that the second term is necessary to get a finite response at  $k = 0$ .

Using these response functions in eq 3.9, we display representative figures illustrating the surface profiles of dilute branched additives to a melt of long linear chains. For stars, we chose  $f = 0.01$  and show the dependence of the surface enrichment on the number of arms,  $p$  (Figure 2a), the length of the arms,  $L$  (Figure 2b), and the strength of the enthalpic contribution to the surface potential for ends,  $\Delta h_e$  (Figure 2c). All figures in this paper, with the exception of Figure 2c, are shown with the surface potentials given by the entropic contribution only; i.e., we choose  $\Delta h = 0$  for all monomers. In Figure 2a, we see that the net entropic attraction for ends (scaling as  $p$ ) dominates over the repulsion of the joint (scaling as  $\log(p)$ ) as  $p$  increases. The repulsion of the joint, however, does produce a maximum away from the wall in the composition profile for values of  $p \geq 4$ .

For combs, we plot in Figure 3 the surface enrichment for various values of the distance  $L$  between junction points, with  $f = 0.01$ ,  $p = 100$ , and  $M = 50$ . Note that for certain combs, the profile exhibits a maximum at a distance  $\sim (Mb^2/6)^{1/2}$ , corresponding to a configuration where an end is adsorbed, while the joints are repelled from the surface. Further below, we will demonstrate how the comb profiles can be fit to a universal curve in an appropriate limit.

#### IV. Blends of Linear and Branched Polymers

As the concentration of the branched species becomes significant compared to that of the long linear chains, the total density is no longer self-consistent with the ground-state potential in which it was calculated. It then becomes necessary to correct the mean-field potential to satisfy the condition of self-consistency. Since these subtle corrections are small in magnitude, a linear response estimate of the necessary correction to the potential, and hence also to the density and concentration profiles, should prove accurate.

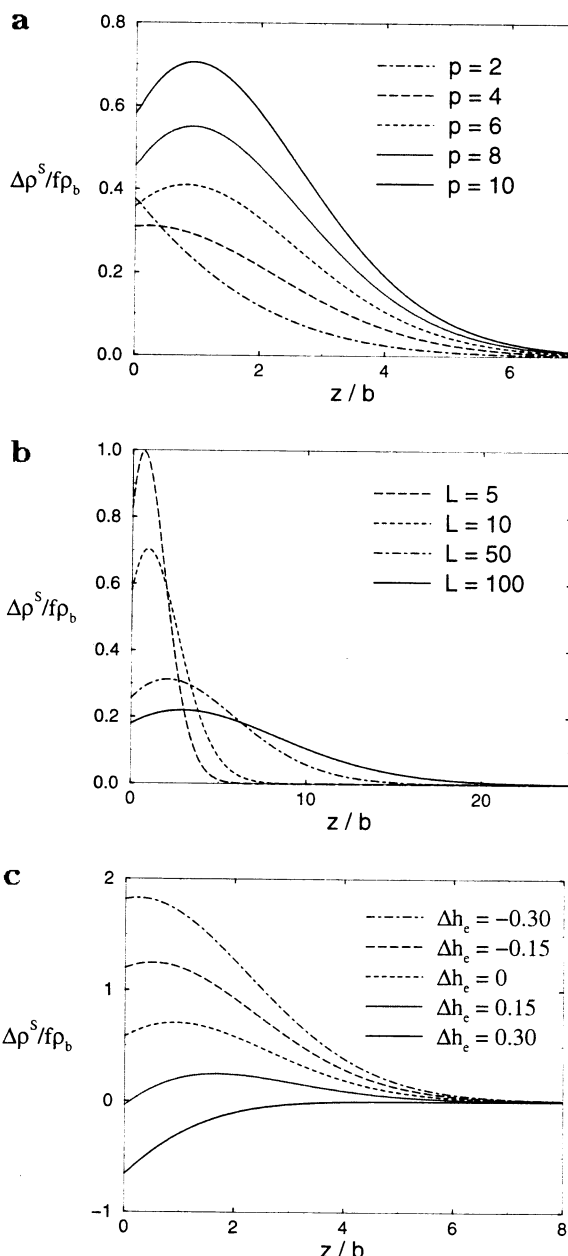


**Figure 2.** Excess monomer density of a dilute ( $f = 0.01$ ) star polymer added to a melt of long linear chains with varying (a) number of arms  $p$ , (b) length of arms  $L$ , and (c) enthalpic end potential  $\Delta h_e$  (given in units of  $k_B T$ ). Unless otherwise stated,  $p = 10$ ,  $L = 10$ , and  $\Delta h_e = 0$ . Note that we have taken  $\xi = 1$  throughout, and so the entropic contributions to the magnitude of the surface potentials are roughly  $T\Delta s_e = 0.307$  and, for  $p = 10$ ,  $T\Delta s_j = -0.787$ .

We designate the previously calculated quantities for the ground-state potential with a subscripted infinity, and the self-consistent quantities after correction without subscripts. Thus for the self-consistent corrections in the density and potential we write

$$\Delta\rho = \rho - \rho_\infty; \quad \Delta U = U - U_\infty \quad (4.1)$$

where

$$U = v\rho; \quad U_\infty = v\rho_{GS} \quad (4.2)$$

The density calculated in the ground-state potential,  $\rho_\infty$ , appearing in eq 4.1 is given by

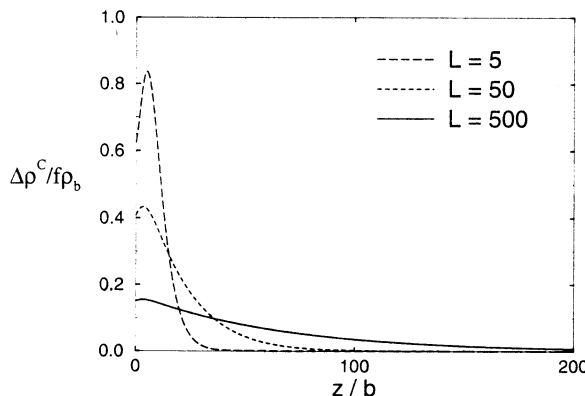


**Figure 3.** Excess monomer density of a dilute ( $f = 0.01$ ) comb polymer with  $p = 100$  teeth of length  $M = 50$  added to a melt of long linear chains with varying distance  $L$  between junction points. Note that we have taken  $\xi = 1$  throughout, and so the entropic contributions to the magnitude of the surface potentials are roughly  $T\Delta s_e = 0.307$  and, for  $p = 3$ ,  $T\Delta s_j = 0.193$ .

$$\rho_\infty(z) = \rho_b + f\Delta\rho_\infty^B(z) \quad (4.3)$$

where  $\Delta\rho_\infty^B(z)$  is just  $\Delta\rho^B(z)$  in eq 3.9. For a change in the potential  $\Delta U$  felt by all monomers, the linear response change in the density is given by (recall  $\Delta U$  is here twice that value used with reflecting boundary conditions response functions in the half-space)

$$\Delta\rho = -S_{\rho\rho}^* \Delta U \equiv - \int_{-\infty}^{\infty} dz' S_{\rho\rho}(z, z') \Delta U(z') \quad (4.4)$$

where

$$S_{\rho\rho} = S_{\rho\rho}^B + S_{\rho\rho}^L \quad (4.5)$$

is the total density-density response function for the blend of both linear and branched molecules, and “\*” denotes the spatial convolution indicated above. Similarly, the change in the density of monomers from either branched polymer or linear polymer alone is given by

$$\begin{aligned} \Delta\rho^B &= -S_{\rho\rho}^B * \Delta U \\ \Delta\rho^L &= -S_{\rho\rho}^L * \Delta U \end{aligned} \quad (4.6)$$

Equations 4.1–4.4 are then solved self-consistently to give

$$\Delta U = [S_{\rho\rho} + v^{-1}]^{-1} * (\rho_\infty - \rho_{GS})$$

for the resulting effective pressure field. (The inverse above denotes a functional inverse taken with respect to the convolution operation “\*”.) The changes in the densities of branched, linear, and all monomers can then be subsequently found by substitution into eqs 4.4 and 4.6. In the limit of incompressibility,  $v \rightarrow \infty$ , we can simplify and write the surface change in the composition  $\Delta\Phi(z)$  as

$$\rho_b \Delta\Phi(z) \equiv \rho^B - f\rho_b = -[\rho^L - (1-f)\rho_b] = \left(\frac{S_{\rho\rho}^B}{S_{\rho\rho}}\right) * S_{pe}^L * U_e^L - \left(\frac{S_{\rho\rho}^L}{S_{\rho\rho}}\right) * (S_{pe}^B * U_e^B + S_{pj}^B * U_j^B) \quad (4.7)$$

where we have allowed for the possibility of a distinct surface potential,  $U_e^L$ , for ends of linear polymers, and now the total density  $\rho = \rho^B + \rho^L = \rho_b$  is a constant. In

the strict limit of absolute incompressibility, the entropic surface fields vanish since they are proportional to the compressibility screening length  $\xi$ . However, even for small but finite compressibilities, and hence finite  $\xi$  and surface fields, eq 4.7 can still be used since it is the leading order expression when  $\xi$  is small compared to the length scales associated with the “pieces” of the branched polymer,  $(Lb^2/6)^{1/2}$  and  $(Mb^2/6)^{1/2}$ . Hence, for the figures displayed in this paper, we have taken  $\xi = 1$  throughout.

The total integrated surface adsorption can be calculated by taking  $1/2$  the limit of  $k = 0$  in the Fourier transform of the equation above, and is found to be

$$\rho_b \int_0^\infty dz \Delta\Phi(z) = \rho_b \left[ \frac{1}{fN^B} + \frac{1}{(1-f)N} \right]^{-1} \left( \frac{2}{N} U_e^L - \frac{n_j^B}{N^B} U_j^B - \frac{p}{N^B} U_e^B \right) \quad (4.8)$$

where  $N^B$  is the total number of monomers in the branched molecule; i.e.,  $N^S = pL$  for a star polymer, and  $N^C = pM + (p-1)L$  for a comb.  $n_j^B$  is the number of joints on the polymer ( $n_j^B = 1$  for a star and  $n_j^B = p$  for a comb). Thus we see that while the total response is proportional to a monomer-fraction weighted molecular weight, the effective weighting of each surface potential is inversely proportional to the molecular weight of that species (a result of the pressure field arising from incompressibility).

From this, we can also have some idea of the range of validity for these linear response approximations: taking an example case of  $f \sim (1-f)$ ,  $N \sim N_B$ , and  $U_e^L \sim U_e^B$ , we find a normalized integrated excess on the order of  $pU_e^B$  for a star and  $p(U_e^B + U_j^B)$  for a comb. Assuming this excess is distributed over a spatial range of order  $(N/p)^{1/2}$  (at least), as would be the case for a star, or of order,  $N^{1/2}$ , as would be the case for a short-branched comb, we find as criteria  $U_e^B < N^{1/2}/p^{3/2}$  and  $(U_e^B + U_j^B) < N^{1/2}/p$  to be in the linear regime for stars and combs, respectively. Thus our results here should be valid for branched polymers for long enough “pieces”.

In Figure 4 we illustrate how the composition profiles change as the molecular weight of the linear chains,  $N$ , and the branched monomer mole fraction,  $f$ , vary for a star/linear blend. It can be seen that the relative molecular weights of the components in a blend play a significant role in determining the pressure fields required to maintain incompressibility, and hence in determining which species is found segregated to the surface. In particular, a lower molecular weight species will incur less of a pressure-induced free energy penalty for an equivalent adsorbed amount. For this reason, there is a tendency toward favoring the smaller species at the surface, which may compete against or enhance any segregation effects due to (entropic or enthalpic) surface potentials. Thus, in Figure 4a, when the arms of the star are the same size as a single linear polymer, the stars are depleted at the surface. For equal total molecular weight,  $N = pL$ , the stars are enriched. Moreover, the length scale of the enrichment is no longer the bulk radius of gyration of either the branched or the linear polymer, but an intermediate length scale which is determined by the pressure field. Additionally, we see in Figure 4b that the surface enrichment is nonmonotonic with the bulk monomer fraction and is peaked near  $f = 0.5$ .

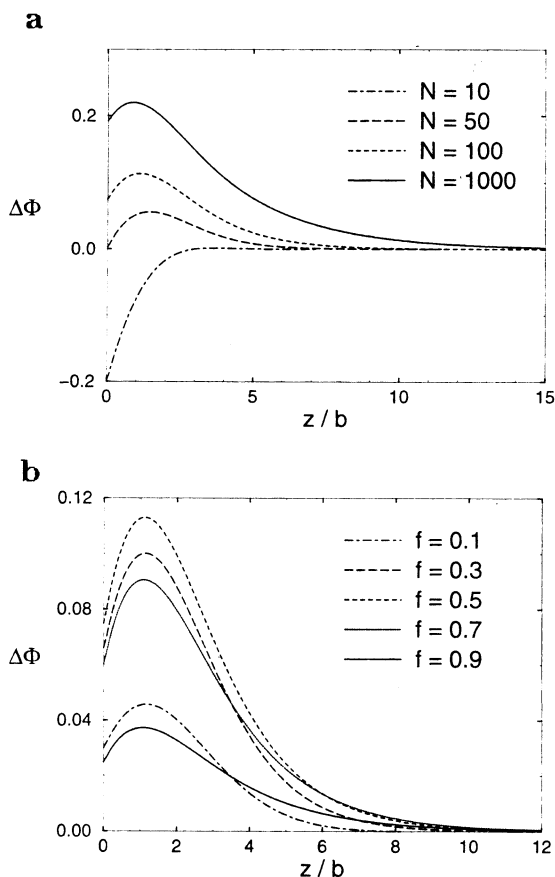


**Figure 4.** Composition profiles in a blend of 10-arm stars (with  $L = 10$ ) and linear polymers for various values of (a) the lengths  $N$  of the linear chains (with  $f = 0.5$  held fixed) and (b) the mole fraction  $f$  of star monomers (with  $N = 100$  held fixed).

These effects can also be seen in Figure 5, where we plot the composition profiles of comb/linear blends versus  $f$ , for the cases of (a) equal molecular weights,  $N = pL + (p - 1)M$ , and (b) much longer linear chains. Of particular note is that in the melt of much longer linear chains, the surface enrichment continues to increase with comb fraction, up to  $f = 0.7$ , as compared to around  $f = 0.5$  for the equal molecular weight blend.

## V. Surface Profile Scaling for Coarse-Grained Combs

Here we develop a coarse-grained description of combs in the limit where the backbone is much longer than the teeth and demonstrate that the surface composition profiles can be fit to a universal curve by an appropriate scaling of the parameters of the blend and branched polymer architecture. In this limit, we imagine that at a length scale greater than the size of the teeth, the comb resembles a linear polymer that occupies extra volume and carries an extra surface interaction (due to the teeth) per backbone monomer, as compared to a linear polymer.

**Coarse-Graining Procedure.** We introduce the coarse-graining by partitioning the polymer into what we will call “blobs”. As illustrated in Figure 6, each blob contains a tooth and a connecting stretch of backbone between joints. (For the purposes of coarse-graining, we can safely ignore the last tooth: accounting for this end effect is straightforward, but tedious and distracting.) With this definition, the comb density/density response functions can be exactly rewritten as

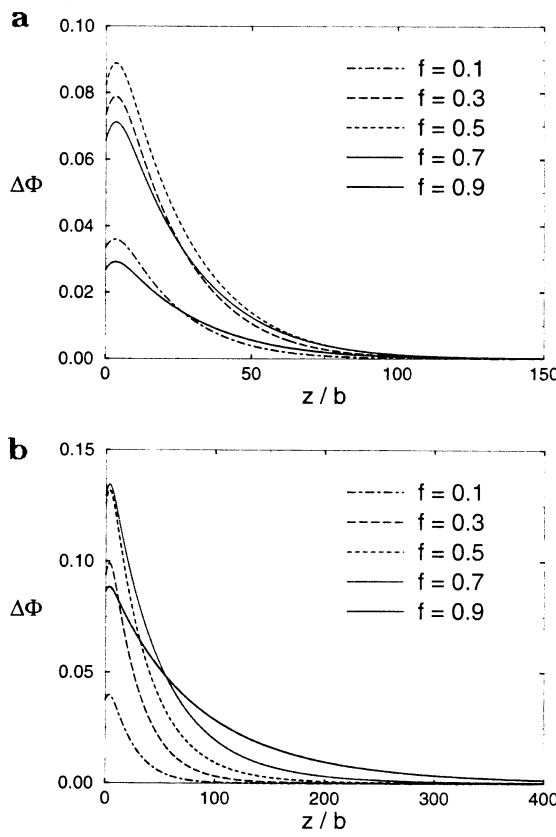


**Figure 5.** Density profiles in a comb ( $p = 100, L = M = 50$ )/linear blend for various values of the comb mole fraction,  $f$ , for the case of (a) equal molecular weights,  $N = pL + (p - 1)M = 9950$  and (b) much longer linear chains,  $N = 500\,000$ .

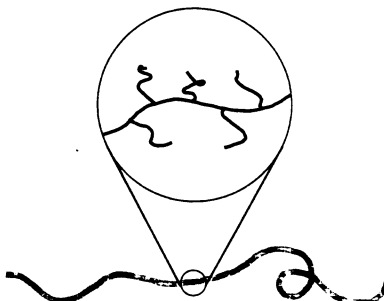


**Figure 6.** Coarse-grained description of a comb polymer as a thicker linear polymer.

$$\hat{S}_{\rho\rho}^C = \frac{f\rho_b}{p(L+M)} \times \left\{ pg^{\text{blob}}(k) + h_L(k)h_R(k) \left[ 2\left(\frac{p}{1-l} - \frac{1-l^p}{(1-l)^2}\right) \right] \right\} \quad (5.1)$$

where

$$g^{\text{blob}}(k) = (L+M)^2 g_D[(L+M)k^2 b^2 / 6] \quad (5.2)$$

represents the response of a single blob, and the left and right connecting functions are given by

$$h_L(k) = (L+M)g_e[(L+M)k^2 b^2 / 6]$$

$$h_R(k) = Lg_e[Lk^2 b^2 / 6] + Mg_e[Mk^2 b^2 / 6] \quad (5.3)$$

The fraction multiplying  $h_L h_R$  in eq 5.1 is a discrete version of the Debye function and has the property

$$2\left(\frac{p}{1-l} - \frac{1-l^p}{(1-l)^2}\right) \rightarrow p^2 g_D(pLk^2b^2/6) \quad (5.4)$$

for  $k^{-1} \gg (Lb^2/6)^{1/2}$ .

For lengths larger than the radius of gyration of the blob, we find

$$g_{\rho\rho}^{\text{blob}} \approx h_L h_R \approx (L + M)^2 \quad (5.5)$$

and thus for  $k^{-1} \gg [(L + M)b^2/6]^{1/2}$ , we find to lowest order in  $1/p$

$$\hat{S}_{\rho\rho}^C \approx f\rho_b p(L + M)g_D(pLk^2b^2/6) \quad (5.6)$$

i.e., the response function in eq 3.19 for a linear chain with the same backbone length,  $pL$ , but with an amplitude proportional to the molecular weight,  $p(L + M)$ , of the whole comb molecule, and not just that of the backbone ( $pL$ ). By a similar procedure, one can determine the coarse-grained end and joint response functions. They are

$$\hat{S}_{e\rho}^C \approx \hat{S}_{j\rho}^C \approx f\rho_b p g_D(pLk^2b^2/6) = \frac{1}{L + M} \hat{S}_{\rho\rho}^C \quad (5.7)$$

which is to say that ends and joints are indistinguishable when coarse-grained over a blob. Furthermore, the response function is proportional to the density/density response function, but with only one monomer of the blob contributing to the response.

**Surface Profile Scaling.** Using eqs 5.6 and 5.7 for the coarse-grained response functions in eq 4.7, we can determine scaling parameters for the surface enrichment profile. In the limit  $N, pL \gg L + M$ , we find for  $k^{-1} \gg [(L + M)b^2/6]^{1/2}$

$$\rho_b \Delta \Phi(\mathbf{r}) \approx -\frac{1}{L + M} S_{\text{RPA}}^C(\mathbf{r}, \mathbf{r}') * [U_j^C(\mathbf{r}') + U_e^C(\mathbf{r}')] \quad (5.8)$$

where the coarse-grained response function is given by the Fourier transform of the familiar RPA expression

$$\begin{aligned} S_{\text{RPA}}^C &= \left[ \frac{1}{\hat{S}_{\rho\rho}^L} + \frac{1}{\hat{S}_{\rho\rho}^C} \right]^{-1} \\ &\approx \left[ \frac{k^2 b^2 / 12 + N^{-1}}{(1-f)\rho_b} + \left( \frac{L}{L+M} \right) \frac{k^2 b^2 / 12 + (pL)^{-1}}{f\rho_b} \right]^{-1} \end{aligned} \quad (5.9)$$

but has an accompanying weighting factor of  $1/(L + M)$  accounting for the density of surface-active sites on the comb. In eq 5.8, we have neglected the term involving the potential for ends of linear chains, as this response is smaller by a factor of  $1/p$ .

The approximate expression for  $S_{\text{RPA}}^C$  in 5.9 (resulting from the standard Lorentzian approximation<sup>12</sup> for the Debye function) allows us to identify

$$\xi_{\text{RPA}} = \left[ \frac{p(L + fM)b^2/6}{fp(L + M)/N + (1-f)} \right]^{1/2} \quad (5.10)$$

as the characteristic length scale for the surface enrichment profile

$$\rho_b \Delta \Phi(z) \approx -A(U_j^C + U_e^C)F(z/\xi_{\text{RPA}}) \quad (5.11)$$

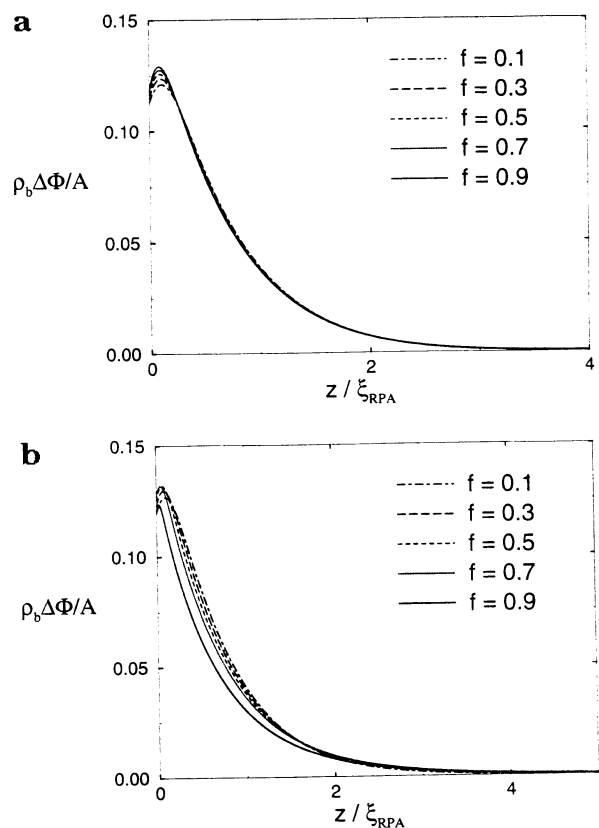


**Figure 7.** Universal fit of the surface composition profiles for the comb/linear blends shown in Figure 5. (a) Case of equal molecular weights; amplitude is scaled by  $A = f(1 - f)p/\xi_{\text{RPA}}$ . (b) Case of much longer linear polymers; amplitude is scaled by  $A = fp/\xi_{\text{RPA}}$ .

where

$$A = f\rho_b \frac{p}{\xi_{\text{RPA}}} \left[ 1 + \frac{fp(L + M)}{(1-f)N} \right]^{-1} \quad (5.12)$$

is an amplitude factor, and

$$F(z/\xi_{\text{RPA}}) = \frac{S_{\text{RPA}}^C(z)}{A(L + M)} \approx e^{-z/\xi_{\text{RPA}}} \quad (5.13)$$

is a profile shape function which is normalized to unity at  $z = 0$ . The last approximation results from the fitting of  $\hat{S}_{\text{RPA}}^C$  in eq 5.9 to an Ornstein-Zernicke form.

In the limit of  $N \rightarrow \infty$ , we find the simplified expressions

$$\rho_b \Delta \Phi \approx -(U_j^C + U_e^C) f \rho_b \frac{p}{\xi_{\text{RPA}}} F(z/\xi_{\text{RPA}}) \quad (5.14)$$

where now

$$\xi_{\text{RPA}} \approx \left[ \frac{p(L + fM)b^2/6}{1-f} \right]^{1/2} \quad (5.15)$$

In Figure 7a, we replot the data of Figure 5a (for several blends of comb polymers with very long linear polymers) onto a universal curve, using the scaling functions given in eqs 5.14–5.15 above.

For the case of equal molecular weights,  $N = p(L + M)$ , we find

$$\rho_b \Delta \Phi \approx -(U_j^C + U_e^C) f(1-f) \rho_b \frac{p}{\xi_{RPA}} F(z/\xi_{RPA}) \quad (5.16)$$

where now

$$\xi_{RPA} \approx [p(L + fM)b^2/6]^{1/2} \quad (5.17)$$

Using the above scaling functions, Figure 7b replots the data of Figure 5b (for various equal molecular weight comb/linear blends) collapsed onto a universal curve.

In the cases above, we find that the characteristic enrichment length,  $\xi_{RPA}$ , is proportional to the square root of  $p(L + fM)$ , which interpolates between the molecular weight of the backbone,  $pL$ , and the total molecular weight of the comb,  $p(L + M)$ , with the weighting factor between the two given by the comb monomer fraction,  $f$ . For dilute concentrations of comb,  $\xi_{RPA}$  scales with the backbone  $R_g$ , but at high concentrations of comb polymer it scales as the  $R_g$  of a linear polymer of the same weight,  $p(L + M)$ . In the latter case, the enrichment becomes controlled by the displacement of linear chains away from the comb-rich surface layer.

**Effective  $\epsilon$  Parameter.** The description above suggests that at a coarse-grained level, it is sufficient to describe a comb polymer with only two architectural parameters: the radius of gyration and the total molecular volume of the comb. Such a reduced description has been used for conformationally asymmetric blends of linear polymers,<sup>2</sup> where the degree of conformational asymmetry is given by

$$\epsilon = \left( \frac{\beta_1^L}{\beta_2^L} \right)^2 \quad (5.18)$$

where

$$(\beta_i^L)^2 \equiv \frac{(R_{g,i})^2}{N_i v_{m,i}} = \frac{b_i^2}{6v_{m,i}} \quad (5.19)$$

are pure-component parameters for the two linear components labeled by  $i$ . In this system, the composition profile for the case of equal molecular weights and small conformational asymmetry is found to be<sup>2</sup>

$$\rho_b \Delta \Phi(z) \equiv \rho_2 - f \rho_b \approx - \rho_b (1-\epsilon) f (1-f) \frac{R_g}{\xi \pi^{1/2}} F_p(z/R_g) \quad (5.20)$$

This can be compared with eq 5.16 above for an equal molecular weight linear/comb blend, where small conformational asymmetry corresponds to the case of small teeth,  $M \ll L$ , which also implies that the length  $\xi_{RPA}$  approaches  $R_g$ . In particular, eq 5.16 can be exactly recovered (again to lowest order in  $M/L$ ) if we make the association

$$(1-\epsilon) \equiv \frac{6\pi^{1/2} \xi (U_j^C + U_e^C)}{L b^2} \quad (5.21)$$

in eq 5.20. In the absence of selective enthalpic surface interactions, we can use eq 3.7 for the entropic potentials  $U_j^C$  and  $U_e^C$  to find the correspondence

$$(1-\epsilon) \equiv - \frac{6\pi^{1/2} (c_3 + c_1) (\xi/b)^2}{L} \quad (5.22)$$

In other words, where the amplitude of the segregation was controlled by the parameter  $(1-\epsilon)$  in the case of conformationally asymmetric blends, for combs it is rather (up to factors of order unity) the density of teeth along the backbone,  $1/L$ . To lowest order in  $M/L$ , a tooth acts to provide a certain coarse-grained attraction to the surface, independent of tooth length. (The tooth length  $M$  can matter if the teeth are made of different monomers than the backbone.) Otherwise, we have the same scaling in both systems with the polymerization index  $p$  and the comb monomer fraction  $f$ .

Finally, we note that our analysis with the coarse-grained response functions in this section applies equally well to conformationally asymmetric blends of linear polymers. (While the linear polymer with the smaller  $\beta$  parameter can in a sense be considered a limiting "microbranched" comb, the actual value of  $\epsilon$  will rely on monomer shapes, bond angles, etc., and not just simple parameters such as  $L$  and  $M$ .) In particular, a composition-dependent length scale  $\xi_{RPA}$  will be found [using a correspondence such as eq 5.21] in the cases of strong segregation or unequal molecular weights (which were not considered in detail in ref 2).

## VI. Rings: Topological Enrichment without End/Joint Effects

After the discussion above, one might arrive at the conclusion that selective surface interactions, either entropic or enthalpic in origin, with architecturally distinctive units (ends or joints) are necessary for polymer architecture to play a role in surface segregation. Intriguingly, however, the topological constraint of a loop alone, *without any preferential surface interaction*, will cause an enrichment of loops at the surface. This phenomenon is a simple, yet direct, consequence of effective reflecting boundary conditions on the polymer propagator under (nearly incompressible) melt conditions close to a surface.

For simplicity, we first consider the case of a single ring polymer of length  $L$  added to a melt of long linear chains. The background melt again serves to create a ground-state potential with a surface depletion region that precisely screens the wall repulsion, and sets up reflecting boundary conditions for stretches of chain long enough to span a distance  $\xi$  and at distances greater than  $\xi$  from the wall. In particular, for linear chains we find

$$P^L(z, z'; s) = \frac{1}{V} G_{\text{refl}}(z, z'; s) \quad (6.1)$$

for the joint probability density of finding monomer  $s$  at position  $z'$  and monomer 0 at  $z$ . (We use translational invariance in the monomer index to write  $G_{\text{refl}}(z, z'; s)$  in place of  $G_{\text{refl}}(z, z'; s, 0)$ .)

If we now consider holding fixed two given points on a ring polymer, each of the two intervening lengths of polymer will fluctuate in the ground-state potential above. For each length of polymer, then, the weight of a given configurational path is the same as that for a stretch of linear polymer of the same length. Integrating over the paths of this intervening stretch (and ignoring crossability constraints) thus reproduces the linear chain propagator. The probability of finding the two chosen points on the ring at the two selected points in space is then proportional to the product of the weights associated with the two stretches of linear chains comprising the ring. The proportionality factor, which can be determined by integration over the posi-

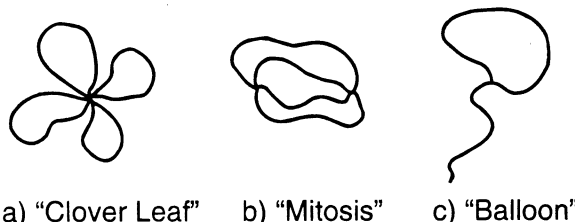
n  
f  
s  
h  
a  
n  
h  
t  
e  
  
-  
y  
r  
r  
g  
y  
t  
a  
d  
f  
  
e  
r  
y  
r  
-  
t  
-  
e  
-  
t  
e  
r  
  
s  
1  
  
1  
f  
1  
e  
3  
3  
r  
  
6

Figure 8. Examples of multiple-loop polymers studied: (a) "clover leaf"; (b) "mitosis"; (c) "balloon".

tions of both fixed monomers and normalizing to unity, is found simply to be the probability,  $1/(2\pi L)^{1/2}$ , of a linear chain assuming a circular configuration. This leads to

$$P^R(z, z'; s) = \frac{(2\pi L)^{1/2}}{V} G_{\text{refl}}(z, z'; s) G_{\text{refl}}(z, z'; L-s) \quad (6.2)$$

as the probability for a ring having monomer  $s$  at position  $z'$  and monomer 0 (which is also monomer  $L$ ) at  $z$ . Integration over  $z'$  yields

$$\rho^R(z) = \frac{1}{V} (1 + e^{-6z^2/Lb^2}) \quad (6.3)$$

for the probability of finding monomer 0 (or any monomer, as they are all equivalent) at position  $z$ .

Thus we find a precise factor of 2 enhancement in ring density at the surface compared to the density in the bulk. Unlike the case of ends and joints, the attraction of the ring to the wall is *independent* of the density healing length,  $\xi$ , as it does not rely upon an entropic preference of ends or joints within the surface layer. Moreover, the surface enhancement factor is independent of ring molecular weight, although the range of enrichment is proportional to the radius of gyration of the ring polymer. Ultimately, for higher bulk densities of ring polymer, the surface excess will be damped by a pressure field arising from the constraint of incompressibility.

That reflecting boundary conditions favor rings at the surface can be understood from consideration of the distribution of linear chains in a melt at a surface. There, reflecting boundary conditions imply that chain configurations are reflected additively about the surface in the counting of statistical weight. Hence, near the surface, chains tend to be compressed (by roughly a factor of 2) along the surface normal, as compared to their average size in the bulk. Therefore, a linear chain has twice the probability of returning to its starting point at the surface compared to in the bulk.

While we do not present here a systematic analysis of various loop architectures (multiple loops in differing topologies), we do discuss three examples, depicted in Figure 8, to explore the effect of multiple loops. The statistical weight of any given polymer configuration with joints or nodes held fixed is given by a product of the reflecting boundary conditions Green's function for each connecting stretch of polymer. As above for the ring, this weight can then be normalized by integrating over all positions of the nodes. The density, say of a particular node, can then be determined by integrating over the positions of all other nodes. Note that integrating over the configurations of stretches of polymer that terminate in a free end results only in a constant (spatially homogeneous) factor, and can thus be ignored for the purposes of determining the surface enrichment of the rest of the polymer.

Using this method, we have found that for both cases a and b of multiple loops examined (Figure 8), the surface enhancement factor of the node is  $2^l$ , where  $l$  in this expression is the number of loops in the polymer (which can be counted as the minimum number of cuts required to remove all closed paths). This can be understood in terms of each additional loop imposing a requirement on a stretch of polymer to return to a given point. At the reflecting surface, the weight for return is double what it is in the bulk. While for the simple ring, all monomers are equivalent and have the same density profile; for multiple loops, the circular symmetry is broken, and the surface enhancement profile for a particular monomer will depend on its distance from the nodes. Thus, for example in case c, an otherwise linear polymer that terminates in a loop will have the loop monomers enriched by a factor of 2 at the surface, but the enhancement factor for monomers along the rest of the linear polymer will diminish as the monomer is more distant from the loop.

## VII. Discussion and Conclusions

We have applied our knowledge of effective boundary conditions and surface potentials for melts of linear chains to molten branched polymers. Using linear-response corrections for induced pressure fields, we have calculated surface composition profiles for a variety of branched polymer blends. Highlighted is the role of the degree of branching and its competition with a pressure-induced molecular weight effect in determining the amplitude and length scale of surface enrichment. Our findings generally indicate that branching produces surface-active ends and junctions; ends are attracted and junctions are repelled from the surface by entropic forces that prove to be universal in character. A recent numerical study using a related self-consistent field approach<sup>19</sup> has reached similar general conclusions and, moreover, gives results and trends which can be quantitatively explained using the analytical results in this paper. Enthalpic interactions may either reinforce or compete with these entropic effects. Regardless of the microscopic origin of the surface selectivity, our formalism should provide a quantitative means of describing surface enrichment.

For blends of comb and linear polymers, we identify a scaling form for the surface composition profile in the limit where the comb polymer can be sensibly coarse-grained as a "thicker" linear polymer with a different effective " $\beta = [L/(L + M)]^{1/2}\beta^L$ " parameter (that used to describe conformationally asymmetric blends). For the case of small conformational asymmetries,  $\beta^L - \beta \ll \beta$ , and equal molecular weights, the amplitude of the entropically driven surface segregation is found to be proportional to the backbone density of teeth. This is in contrast to the result for the conformationally asymmetric blends of linear polymers,<sup>2</sup> where the segregation is governed by the conformational asymmetry parameter  $\epsilon$ , which is given by the ratio of the squared pure-component  $\beta^L$  parameters. In a sense, while the limit of short teeth corresponds to a "microbranched" polymer, a determination of the  $\beta^L$  parameter (which controls  $\epsilon$ ) depends on geometrical considerations based on the shape of the monomer, and their relative allowed conformations.

Nonetheless, with a comb analog for the  $\epsilon$  parameter, we have identified a continuous variable for the control of surface segregation by manipulation of branch content. In our earlier study of conformationally asym-

metric blends, it was found that very small differences in  $\beta$  could lead to strong surface segregation. By controlling the number, length of, and distance between teeth on a comb polymer, we can exercise a greater degree of control over the range from weak to strong surface segregation.

Given that surface segregation of stars and combs was found to be controlled by effective surface potentials for ends or joints, it is remarkable to note that polymers with loops can segregate to the surface from topological considerations alone. For a dilute amount of rings added to a melt of longer polymers, the surface density of ring monomers is *precisely doubled* relative to the bulk. Moreover, the magnitude depends neither on  $\xi$  (as it does not rely on variations in the density), nor on the chain length of the ring, and is hence purely a consequence of the ring topology. Multiple rings further double the surface enhancement factor. This striking prediction results from the incompressibility-induced reflecting boundary conditions at the surface, and may serve as a distinctive experimental or simulation test of such statistics. Moreover, surface enhancement of rings may affect the kinetic processes during ring polymerization, or in self-assembling/living polymer systems.

**Acknowledgment.** This work was supported by the MRL program of the National Science Foundation under Award No. DMR-9123048.

## References and Notes

- (1) Binder, K. *Acta Polym.* **1995**, *46*, 204.
- (2) Wu, D. T.; Fredrickson, G. H.; Carton, J.-P. *J. Chem. Phys.* **1996**, *104*, 6387.
- (3) Yethiraj, A. *Phys. Rev. Lett.* **1995**, *74*, 2018.
- (4) Donley, J. P.; Wu, D. T.; Fredrickson, G. H. Manuscript in preparation.

- (5) (a) Kumar, S. K.; Yethiraj, A.; Schweizer, K. S.; Leermakers, F. A. M. *J. Chem. Phys.* **1995**, *103*, 10832. (b) Yethiraj, A.; Kumar, S. K.; Hariharan, A.; Schweizer, K. S. *J. Chem. Phys.* **1994**, *100*, 4691. (c) Carignano, M. A.; Szleifer, I. *Europhys. Lett.* **1995**, *30*, 525.
- (6) (a) Scheffold, F.; Budkowski, A.; Steiner, U.; Eiser, E.; Klein, J.; Fetter, L. *J. J. Chem. Phys.* **1996**, *104*, 8795. (b) Steiner, U.; Klein, J.; Eiser, E.; Budkowski, A. *Science* **1992**, *258*, 1126. (c) Steiner, U.; Klein, J.; Fetter, L. *J. Phys. Rev. Lett.* **1994**, *72*, 1498.
- (7) (a) Karim, A.; Singh, N.; Sikka, M.; Bates, F. S. *J. Chem. Phys.* **1994**, *100*, 1260. (b) Sikka, M.; Singh, N.; Karim, A.; Bates, F. S.; et al. *Phys. Rev. Lett.* **1993**, *70*, 307.
- (8) Fredrickson, G. H.; Liu, A. J.; Bates, F. S. *Macromolecules* **1994**, *27*, 2503.
- (9) Fredrickson, G. H. *Macromolecules* **1994**, *27*, 7382.
- (10) (a) Helfand, E.; Tagami, Y. *J. Chem. Phys.* **1972**, *56*, 3592. (b) Helfand, E.; Tagami, Y. *J. Chem. Phys.* **1972**, *57*, 1812.
- (11) (a) Helfand, E. *J. Chem. Phys.* **1975**, *62*, 999. (b) Helfand, E.; Sapse, A. M. *J. Chem. Phys.* **1975**, *62*, 1327.
- (12) Doi, M.; Edwards, S. F. *The Theory of Polymer Dynamics*; Clarendon: Oxford, 1986.
- (13) Wu, D. T.; Fredrickson, G. H.; Carton, J.-P.; Ajdari, A.; Leibler, L. *J. Polym. Sci., Part B: Phys. Ed.* **1995**, *33*, 2373.
- (14) Edwards, S. F.; Olvera de la Cruz, M. In *Quantum Field Theory and Quantum Statistics*; Batalin, I. A., Isham, C. J., Vikovisky, G. A., Eds.; Taylor and Francis: Philadelphia, 1987.
- (15) Schweizer, K. S. *Macromolecules* **1993**, *26*, 6050.
- (16) (a) Elman, J. F.; Johs, B. D.; Long, T. E.; Koberstein, J. T. *Macromolecules* **1994**, *27*, 5341. (b) Jalbert, C.; Koberstein, J. T.; Yilgor, I.; Gallagher, P.; Krukonis, V. *Macromolecules* **1993**, *26*, 3069. (c) Sauer, B. B.; Dee, G. T. *J. Colloid Interface Sci.* **1994**, *162*, 25.
- (17) The surface potentials  $U(z)$  used in this paper, such as those defined in eq 3.8, represent physical free energy differences, and are therefore convoluted with the *reflecting* boundary condition response functions. In ref 13, we defined the  $U(z)$  to correspond to *twice* the physical free energy difference, since these were to be convoluted with the *free* response functions.
- (18) Morse, D.; Fredrickson, G. H. *Phys. Rev. Lett.* **1994**, *73*, 3235.
- (19) Walton, D. G.; Mayes, A. M. Preprint.

MA9602278